DOI: 10.1021/ma101473r

Macromolecules
ARTICLE

Thermal Behavior of Poly(L-lactide) Having Low L-Isomer Content of 94% after Compressed CO_2 Treatment

Qiaofeng Lan,[†,§] Jian Yu,*[,†] Jiasong He,[†] Frans H. J. Maurer,[‡] and Jun Zhang[†]

[†]*Beijing National Laboratory for Molecular Sciences (BNLMS), Key Laboratory of Engineering Plastics, Joint Laboratory of Polymer Science and Materials, Institute of Chemistry, Chinese Academy of Sciences, Beijing 100190, China,* [‡]*Department of Polymer & Materials Chemistry, Lund Institute of Technology, Lund University, SE-22100 Lund, Sweden, and* [§]*Graduate School of Chinese Academy of Sciences, Beijing 100039, China*

Received July 2, 2010; Revised Manuscript Received September 16, 2010

ABSTRACT: The effect of compressed CO_2 treatment on the thermal behavior of poly(L-lactide) (PLLA) with low L-isomer content of 94% was studied by using differential scanning calorimetry (DSC) and temperature modulated DSC. It was shown that the treated samples displayed rich thermal transition signals during DSC heating, which is differ from the PLLA having high L-isomer content, including enthalpy relaxation, endothermic annealing, melting−recrystallization process, and cold crystallization. The results suggested that the crystalline phase obtained has less perfection and low crystallinity regardless of the treatment conditions because of the low crystallizability of the PLLA. This PLLA was induced to crystallize after treatment under CO_2 at 2 MPa and temperature ≥ 65 °C and at pressures of 4−16 MPa and temperatures as low as 0 °C. At 2 MPa, the α crystal form is formed predominantly in the crystallized samples. The results also indicated that the PLLA−CO_2 system exhibited the property of retrograde vitrification.

Introduction

Poly(L-lactide) (PLLA) draws currently great attention from both scientific and technological areas due to its biodegradability and biocompatibility. PLLA is a semicrystalline polymer, and its thermal behavior has been studied extensively in terms of physical aging, cold crystallization, multiple melting, polymorphism, and crystal form transition. Most of these studies have been focused on the optically pure PLLA with high molecular weight, which have melting points (T_m) typically in the 160−180 °C range and enthalpies of melting of 40−50 J/g depending on the processing conditions. It have been shown that the molecular structure, such as chemical composition, molecular weight, and molecular weight distribution, and processing parameters can influence the solid state structure of PLLA, which determines a number of its physical properties and applications.[1−13]

In recent years, the interactions between PLLA and CO_2 have attracted wide attention. CO_2 has low-cost, nontoxic, nonflammable, and environmentally friendly properties. Moreover, CO_2 can dissolve in amorphous phase of polymer to a substantial amount, leading to the dramatic depression of the glass transition temperature (T_g) and T_m of polymers.[14−19] Therefore, potentially harmful organic solvents and high-temperature process can be avoided by using CO_2 as a medium in the synthesis and processing of PLLA, such as polymerization,[20−22] particle formation,[23,24] fiber preparation,[25] and foam and porous polymer fabrication.[26−30]

The effects of supercritical and subcritical CO_2 on the crystallization behavior of PLLA have been studied by several groups to gain in-depth understanding about the relationships between physical properties and polymer processing. The kinetics of crystallization from melt and glassy state were reported in the presence of CO_2 up to 5 MPa by using high-pressure differential scanning calorimetry (DSC).[19,31,32] The crystallization temperature range shifts to lower temperature because T_g and T_m linearly decrease with pressure of CO_2, while the maxima crystallization rate increases obviously.[19,30] The crystallization rate is increased at the temperatures in the crystal growth controlled region and decreased at the temperatures in the nucleation controlled region.[19,32] Because of the strong plasticization effect of CO_2, PLLA can be crystallized under compressed CO_2 even at a low temperature of 0 °C.[33,34] Furthermore, PLLA samples crystallized at 0−10 °C under 7−15 MPa and 0−20 °C under 3 MPa have high transparency comparable to the amorphous one. The reason seems to be that the crystals formed during CO_2 treatment are disorder with the crystalline superstructure on a nanosized scale. It is worth to note that the polymers used in all above-mentioned studies were PLLA with high L-isomer content of at least 98% (optical purity > 96%). The PLLA can be sufficiently crystallized just under CO_2 at 3 MPa and 0 °C for 2 h, exhibiting no cold crystallization behavior during heating.[33] Therefore, when the time, pressure, and temperature were above certain values, the melting behavior of these treated PLLA is almost independent of treatment conditions of compressed CO_2.

In the previous studies, we have investigated the crystallization behavior of polycarbonate (PC) and poly(ethylene 2,6-naphthalate) (PEN), which have slow rate for thermal-induced crystallization due to their chain rigidity, with help of the supercritical CO_2 technique.[35,36] Supercritical CO_2 induced the crystallization of PC under mild conditions to overcome the time-consuming process of thermal crystallization, which was help to study the influence of long-chain branching on the crystallization behavior of PC.[35] For PEN, the crystallization temperature was modulated in a wide range by changing the pressure of supercritical CO_2 and adding a cosolvent, and a diagram of the crystallization of PEN versus temperature, pressure, and solubility parameter of medium was established.[36]

*Corresponding author: Fax +86-10 6261 3251; e-mail yuj@iccas.ac.cn.

 Published on Web 09/30/2010

In general, the crystallization kinetics of PLLA strongly depends on the L-isomer content. The crystallizability of PLLA having low L-isomer content is lower than the ones with high L-isomer content. It was reported that the crystallization half-time increases about 40% for every 1 wt % meso-LA in the copolymerization of L-LA with meso-LA,[37] and the random copolymer of L-LA with 12% meso-LA has maxima spherulite rate growth more than 100 times slower than the L-LA homopolymer.[6] Therefore, the treatment by compressed CO_2 would be an effective method to study the thermal behavior of PLLA having low L-isomer content. PLLA with low L-isomer content would have different crystallization kinetics from those with high L-isomer content in the presence of CO_2, and the treated samples would exhibit variable melting behavior depending on the treatment conditions. As far as we are concerned, there is no study on the thermal behavior of PLLA with low L-isomer content after treatment under compressed CO_2.

In the present study, a commercialized PLLA having relatively low L-isomer content of ca. 94% was used. It can be induced to crystallize in compressed CO_2 in a wide range of treatment conditions. According to the treatment pressures and temperatures, the PLLA sample in compressed CO_2 displayed quiet distinct crystallizability, such as from being amorphous or low crystallinity at the pressure of 2 MPa at 0−50 °C to relatively high crystallinity at higher pressures. Therefore, the relationship between rich thermal transitions of treated PLLA samples and treatment conditions of compressed CO_2 has been examined in detail by using standard DSC and temperature-modulated DSC (TMDSC), including endothermic annealing, cold crystallization, and double melting phenomena. Some particular behaviors for the treated PLLA, which relate with the relatively low L-isomer content, are discussed. The results obtained in this study would facilitate to gain insight into the relationship between physical properties and molecular structures of PLLA.

Experimental Section

Materials and Sample Preparation. Poly(L-lactide) (PLLA) ($M_w = 1.3 \times 10^5$, $M_w/M_n = 1.9$), prepared through ring-opening polymerization of L-LA, was kindly supplied by Zhejiang Hisun Chemical Co. Ltd., China, as commercialized granular pellets. The optical purity was determined to be 88% by optical rotation measurement, i.e., L- and D-isomer contents of PLLA were 94% and 6%, respectively. Among eight possible well-resolved hexad stereosequences with sis and iis/sii core sequences,[38] only the resonance corresponding to iiiss at ~5.208 was present in the homonuclear-decoupled ^{1}H NMR spectrum of the PLLA (see Supporting Information for details). This indicates that the stereosequence distribution of the PLLA is similar to that of random copolymer of L-LA with 12% meso-LA. CO_2 with a purity of 99.95% was supplied by Beijing Analytical Gas Factory, China.

The PLLA were molded by compression at 180 °C into films of 300 μm thickness after drying under vacuum at 60 °C overnight and then quickly quenched to room temperature. The obtained transparent films were cut into specimens with dimensions of 10 × 10 mm for further compressed CO_2 treatment.

Compressed CO_2 Treatment. The PLLA samples were treated by CO_2 at designed temperature and pressure for 2 h in a high-pressure vessel connected to a high-pressure pump, which was flushed with low-pressure CO_2 for about 3 min before pressurization. Then the vessel was depressurized in 1 h. After treatment, all the samples were kept dry at ambient condition for about 2−3 weeks to ensure the total desorption of CO_2 prior to further measurements. For convenience, the code of PLLAx−y was used to represent the sample after treatment under CO_2 at x MPa and y °C for 2 h.

Measurements. A TA Instruments Q-1000 DSC was used for standard DSC and TMDSC analysis. All measurements were carried out with ca. 5 mg samples from 20 to 180 °C under a nitrogen environment. In the standard DSC analysis, a heating rate of 10 °C/min was used unless indicated. The T_g, ca. 56 °C, was taken as the midpoint of the glass transition step in the heat capacity curve for samples quenched from melt at 180 °C for 2 min. The TMDSC measurements were performed with a heating rate of 3 °C/min having an oscillation period of 60 s and amplitude of 0.5 °C. The crystallinity was calculated by using the fusion heat of 93 J/g for 100% crystalline PLLA.[39] The results were analyzed by using Universal Analysis 2000 (ver. 4.5A) of TA Instruments.

XRD analysis was conducted on a Rigaku D/max 2500 with Cu Kα radiation. All patterns were obtained at 40 kV and 300 mA from 5° to 30° with a scanning rate of 1°/min.

Results and Discussion

Optically pure PLLA, i.e., the L-isomer content higher than 98%, is a semicrystalline polymer with slow crystallization rate. Incorporation of stereochemical defects into PLLA further reduces the crystallization rate as well as the melting point and crystallinity.[3,6,37,40,41] It was reported that PLLA would lose its crystallizability when the optical purity was smaller than 76%.[3] In this study, the PLLA polymer with 94% L-isomer content, i.e., an optical purity of 88%, was used. It had low ability to crystallize at ambient pressure, and the crystallization from melt was hindered at a cooling rate as low as 5 °C/min. However, different extents of crystallization were induced by the treatment in compressed CO_2.

Samples Crystallized after Treatment. Figure 1 shows the DSC heating curves for PLLA samples after treatment in compressed CO_2 at 2, 4, 8, and 16 MPa and different treatment temperatures (T_{tr}) for 2 h. The results for the quenched and untreated samples are also present in Figure 1a for comparison. As shown in Figure 1, the samples reveal obvious feature of endothermic peaks and no exothermic one above 80 °C after treatment under CO_2 at 2 MPa and $T_{tr} \geq$ 65 °C or higher pressures and all temperatures studied. This indicates that the crystals corresponding to the melting peaks were induced at T_{tr} as low as 0 °C when the pressure was above 4 MPa. In these samples crystallized after treatment in compressed CO_2, there are up to three endotherms in the DSC curves. In the following discussion, these peaks are denoted as P_1, P_2, and P_3 from low to high temperatures, and the peak temperatures of them are listed in Table 1.

Annealing Peak for Crystallized Samples. P_1 is a small and broad endothermic peak, which is analogous to the well-known annealing peak reported in many semicrystalline polymers, such as isotactic polystyrene,[42−44] poly(phenylene sulfide),[45] poly(ethylene terephthalate),[45] and syndiotactic polypropylene,[46] etc. However, it has never been mentioned for PLLA treated in compressed CO_2.

P_1 has the peak temperature varying in a wide range from 80 to 130 °C according to the treatment conditions. The peak temperature is about dozens degrees above T_{tr} with almost unchanged intensity at a certain treatment pressure. However, the difference between the peak temperatures of P_1 and T_{tr} decreases with increasing T_{tr}, e.g., from about 38 °C for PLLA2−50 to 18 °C for PLLA2−95. Replotted from Figure 1, Figure 2 shows the DSC curves of PLLA samples treated under compressed CO_2 at 65 °C and various pressures. The shift of P_1 to higher temperature with increasing treatment pressure results in a merge of P_1 into P_2 at the lower temperature side for PLLA16−65. On the other hand, P_1 fades away for the samples after treatment at the pressure of 16 MPa, as shown in Figure 1d.

P_1 also varies with testing conditions. Figure 3 shows the DSC curves obtained at heating rates from 5 to 40 °C/min for

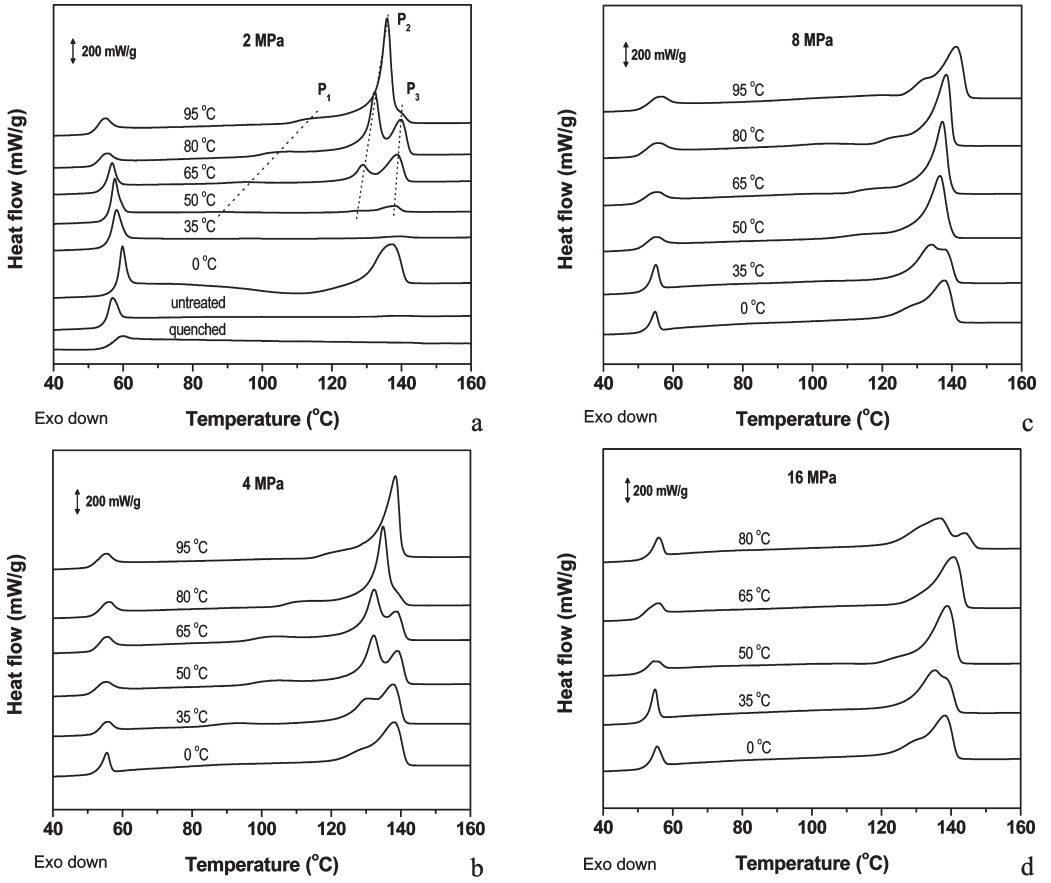

Figure 1. DSC curves for PLLA samples treated under compressed CO_2 at different pressures: (a) 2, (b) 4, (c) 8, and (d) 16 MPa.

Table 1. Summary of DSC Data at the Heating Rate of 10 °C/min for PLLA Samples

	peak temperature (°C)			
sample	P_1	P_2	P_3	ΔH_{total}[a] (J/g)
quenched[b]				
untreated				0.4
PLLA2−0			137.3	0.2
PLLA2−35			139.4	0.2
PLLA2−50	88.2	127.4	138.2	0.4
PLLA2−65	94.7	128.8	138.7	7.7
PLLA2−80	104.5	132.2	140.1	29.5
PLLA2−95	113.1	135.9	shoulder	30.5
PLLA4−0	87.3	127.6	138.1	22.2
PLLA4−35	92.1	129.6	137.8	25.0
PLLA4−50	103.2	132.2	139.4	26.1
PLLA4−65	103.0	132.3	139.1	26.6
PLLA4−80	110.3	134.9	shoulder	28.8
PLLA4−95	shoulder	138.4		29.0
PLLA8−0		shoulder	137.9	22.2
PLLA8−35	103.0	134.1	138.4	22.0
PLLA8−50	113.9	136.5		26.7
PLLA8−65	116.7	137.2		26.6
PLLA8−80	shoulder	138.3		26.4
PLLA8−95	shoulder	141.2		25.1
PLLA16−0		shoulder	138.2	22.0
PLLA16−35		135.4	138.9	22.1
PLLA16−50	shoulder	138.8		24.4
PLLA16−65		140.8		23.3
PLLA16−80		136.9	144.3	21.1

[a] Obtained from TMDSC total heat flow curve. [b] Quenched from melt after 2 min at 180 °C in DSC and then tested with heating rate of 10 °C/min.

PLLA2−65 and PLLA4−65. With increasing heating rate, P_1 shifts to higher temperature with unchanged intensity, indicating a superheating nature of the process related to P_1.

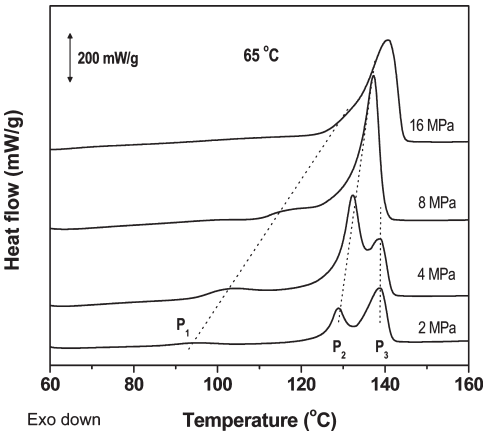

Figure 2. DSC curves for PLLA samples treated under compressed CO_2 at 65 °C and different pressures (replotted from Figure 1).

The annealing peak is suggested to originate from the nonreversible enthalpy relaxation of rigid amorphous fraction, which is a third phase in semicrystalline polymers located in the interface between the crystalline and mobile amorphous phases.[42,43] Consequently, the characteristic of P_1 was further studied by TMDSC. TMDSC is a powerful tool to study complex thermal processes contained in the heat flow curves by separating the total heat flow signals into reversible part relative to heat capacity and nonreversible one resulting from kinetic effects.[47] Therefore, exothermic peaks appear only in the nonreversible curves, and endothermic signals can be detected in both reversible and nonreversible curves.[48,49] Chosen as examples, the total, reversible, and nonreversible heat flow curves of TMDSC for

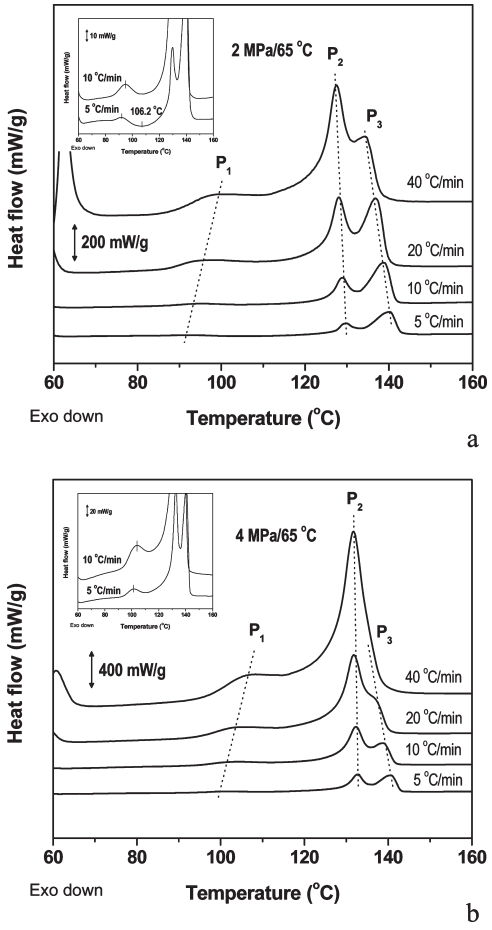

Figure 3. DSC curves at different heating rates for treated PLLA samples: (a) PLLA2−65 and (b) PLLA4−65.

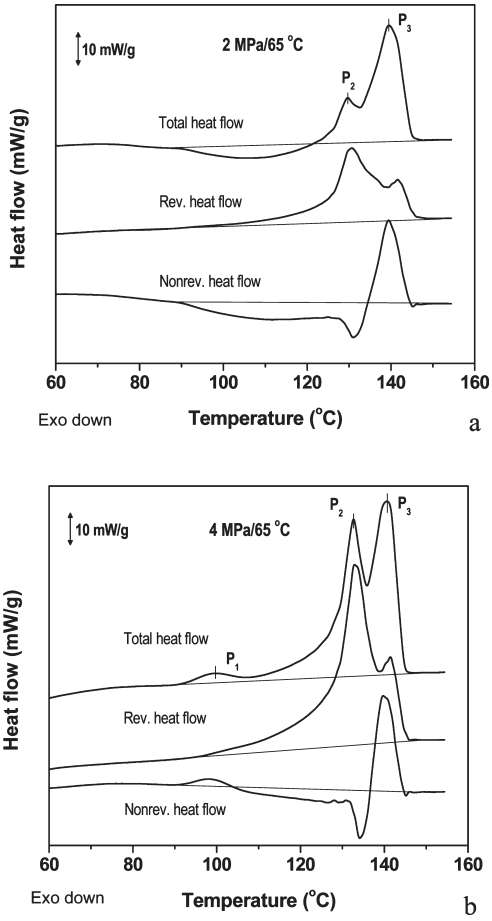

Figure 4. TMDSC curves for (a) PLLA2−65 and (b) PLLA4−65.

PLLA2−65 and PLLA4−65 are shown in Figure 4. Their total heat flow curves are similar to the conventional DSC curves at low heating rate (Figure 3). For PLLA4−65, the total heat flow curve exhibits P_1 at about 100 °C. An endotherm corresponding to P_1 is clearly displayed in the nonreversible heat flow curve, while no endothermic peak is present in the reversible curve in the same temperature range. For PLLA2−65, P_1 disappears in the total curve due to the overlap by a followed exothermic cold crystallization peak, which will be discussed later. The results shown in Figures 3 and 4b confirm that the process related to P_1 has the same nonreversible feature with that of annealing peak, indicating that P_1 is due to the nonreversible relaxation of rigid amorphous phase formed during CO_2 treatment.

Double Melting Peaks for Crystallized Samples. Figures 1 and 2 show that many of PLLA samples crystallized in CO_2 presents double melting endotherms closely in DSC curves. As shown in Table 1, the crystallized samples have T_m in the range from 125 to 145 °C, which are far below typical values of optically pure PLLA in the 160−180 °C range. It is well-known that the T_m of crystallized PLLA greatly depends on the optical composition in polymer,[3,6,40,41] decreasing dramatically with an increase in the D-isomer content because these stereoisomer units would be rejected from the crystal as defects. Being a PLLA with 6% D-isomer, the PLLA used in this study has T_m closer to the random copolymers of L-LA with 12% meso-LA[6] than the one with 6% D-LA,[41] whose T_m were reported in the range of 135−145 and 145−155 °C, respectively. It is consistent with the result disclosed by ^{1}H NMR, indicating that D-isomer units are randomly distributed in the polymer chains unpaired, instead of in pair as in L-LA/D-LA copolymers.

Double melting is a common feature for semicrystalline polymers. For PLLA, it is well accepted that the double melting behavior is associated with the melting−recrystallization process occurred during heating.[3,10,11,50] However, the double melting behavior for the treated PLLA having high L-isomer content in CO_2 is too slight to deserve well-studied.[31−33] In this study, the low melting peak P_2 is related to the crystals formed by the primary crystallization during CO_2 treatment, while the high melting peak P_3 to those reorganized after (partial) melting of original crystals by recrystallization process.

To verify the origin of double melting peaks, the DSC curves conducted at different heating rates are shown in Figure 3. From these curves, it is clear that the relative intensity of P_2 to P_3 increases with increasing heating rate. Meanwhile, the position of P_2 is almost independent of the heating rate, i.e., 128.5 ± 0.9 °C for PLLA2−65 and 132.0 ± 0.5 °C for PLLA 4−65, and P_3 slightly shifts to lower temperature with increasing heating rate and completely combines with P_2 at 40 °C/min for PLLA4−65. These results are compatible with the melting−recrystallization model for double melting behavior of semicrystalline polymers.[51,52] The primary crystallization occurred in a completely unconstrained melt under the assistance of compressed CO_2 to form original crystals. P_2 is attributed to the melting of these crystals presented in the sample, which exhibit similar melting range irrespective of the heating rate in DSC measurement due to their relative high stability and perfection. When the heating rate was lower, there was enough time for

polymer chains, which would obtain increasing mobility by the increase in temperatures to form more perfect crystals related to P_3. In contrast, when the scan rate was higher, structural reorganization was kinetically suppressed. For PLLA4−65, the high stability of original crystals was also unfavorable for the melting−recrystallization process, resulting in a single melting peak at 40 °C/min compared to double peaks for PLLA2−65. On the other hand, secondary crystallization, which generally results in low stability crystals with superheating nature,[35] is excluded in this study to explain the multiple melting behavior.

The TMDSC results shown in Figure 4 further confirm the existence of melting−recrystallization process during heating. In the reversible heat flow curves, double melting peaks can be seen in the range from 90 to 150 °C, corresponding to P_2 and P_3 in the total heat flow curves, respectively. However, the low reversible melting peak is much bigger than P_2, while the high one is smaller than P_3. A sharp nonreversible exotherm with the peak temperature between 130 and 135 °C is present accompanied by P_1 and low reversible endothermic peak, ascribed to the recrystallization. The nonreversible exotherm counteracts the big reversible melting endotherm to result in P_2 having small intensity in the total heat flow curve. As for the nonreversible endotherm ranged from 135 to 145 °C, it represents the nonreversible melting contribution of the recrystallized crystals. In addition, the wide exotherm below 130 °C corresponds to the cold crystallization process during heating, to be discussed later. Therefore, it can be concluded that the melting of original crystals during heating proceeds simultaneously with the cold crystallization and the subsequent recrystallization process to form crystals with higher stability. The melting of recrystallized crystals at higher temperatures includes reversible and nonreversible signals.

As shown in Figures 1 and 2, with increasing T_{tr} and treatment pressure, P_2 moves to higher temperature, and P_3 keeps almost unchanged. Meanwhile, P_2 increases in intensity at the expense of P_3. Consequently, P_3 fades away and merges as shoulder of P_2 at the high temperature side, when the treatment conditions are above a certain T_{tr} and pressure. Higher pressure of CO_2 results in the combination of P_2 and P_3 at lower T_{tr}, i.e., from 95 °C for 2 MPa to 80 °C for 4 MPa, and 50 °C for 8 and 16 MPa, respectively, as shown in Table 1. It is clear that more primary crystals with increasing thermal stability can be formed by increasing T_{tr} and pressure in compressed CO_2 treatment, resulting in the decease of the extent of recrystallization during subsequent heating. Accordingly, the intensity of P_3 decreases as the peak temperature and intensity of P_2 increase.

However, by increasing T_{tr} to 80 °C at 16 MPa, the treated sample exhibits double melting peaks again with the major melting peak moving to lower temperature, as shown in Figure 1d. The degradation of polymer during the treatment can be excluded by thermogravimetric analysis because PLLA16−80 has almost the same weight loss curve with the untreated sample (Figure S2 in the Supporting Information). This downward shift of the major melting peak means some imperfection in the crystallized samples. It is well-known that the melting point of the polymer decreases with increasing pressure of CO_2. If the PLLA sample was molten during compressed CO_2 treatment and crystallization took place from the melt only when the treatment was over, i.e., at lower temperature and/or pressures in a relatively short period of time, these conditions would result in the formation of the crystals with less perfection. Accordingly, we suggest that the T_m of PLLA was reduced from about 140 °C at ambient pressure to below 80 °C at 16 MPa.

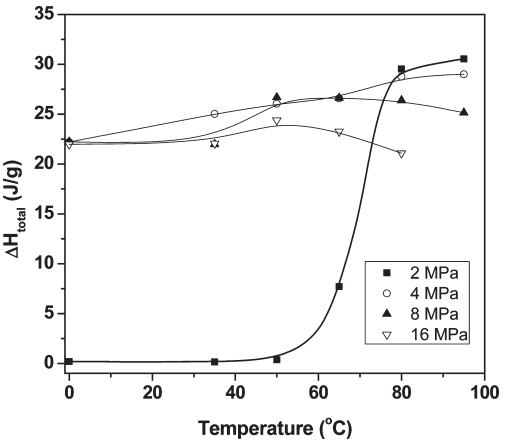

Figure 5. ΔH_{total} for different treated PLLA samples.

The depression of T_m of PLLA is consequently estimated to be above 3.75 °C/MPa in this study, which is higher than 1.76 °C/MPa determined by Lian et al.[53] By combining data from different references[19,54] and their work, Lian et al.[53] reported a linear relationship between T_m of PLLA and CO_2 pressure up to 41.4 MPa. The difference in T_m depression is most probably attributed to the fact that those PLLA samples used in their studies had higher L-isomer contents, indicated by the higher T_m than this used in our study here. The minor stereoisomer units incorporated as stereochemical defects would decrease the equilibrium melting temperature[3,6,40,41] and the fold surface free energy[6] of PLLA, both of which would influence the effect of pressure on the T_m of polymer in the presence of CO_2.

Crystallinity of Crystallized Samples. The total enthalpies of multiple endothermic peaks, ΔH_{total}, are calculated for all treated samples from the TMDSC total heat flow curves. They include P_1, a value less than 1 J/g, due to the severe overlap with P_2.

Figure 5 summarizes the ΔH_{total} for all samples after treatment. For the samples treated at the pressure of 2 MPa, the ΔH_{total} is small at $T_{tr} \leq 50$ °C and increases abruptly to about 29.5 J/g as T_{tr} increases to 80 °C. At higher T_{tr} of 80 and 95 °C, the ΔH_{total} levels off. For the samples treated at the higher pressures, the ΔH_{total} increases slightly with increasing T_{tr}, and the ΔH_{total} is independent of pressure in the range of 4−16 MPa at $T_{tr} \leq 65$ °C. On the other hand, for the samples treated at higher T_{tr} of 80 and 95 °C, the ΔH_{total} decreases with the treatment pressure. In the presence of CO_2, the chain mobility increased significantly from the ambient pressure to 2 MPa. Therefore, the compressed CO_2 accelerated the crystallization of PLLA under same supercooling degree below T_m, and the maximum crystallization rate increased remarkably. On the other hand, with increasing the pressure, the chain mobility did not increase so obviously. The curve of crystallization rate vs temperature for PLLA would move to lower temperature due to the depression of T_g and T_m. Therefore, the crystallization rate was depressed at higher pressures and temperatures just below the real T_m under CO_2 because the conditions were in the nucleation controlled region. Consequently, the crystallinity developed in the samples treated at 80 and 95 °C for limited time period of 2 h decreased with increasing the treatment pressure from 2 to 16 MPa, resulting in low enthalpy. The crystallinities for crystallized samples except PLLA2−65 are 22−33% by using the heat of fusion of 93 J/g for 100% crystalline PLLA.[39] By comparison, the PLLA with similar stereosequence distribution was reported to

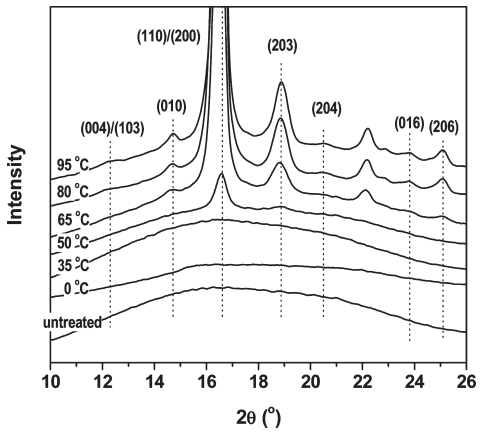

Figure 6. XRD patterns for the PLLA samples treated under compressed CO_2 at 2 MPa and different temperatures.

have quite low crystallinities after complete crystallization, i.e., $<20\%$ for random copolymer of L-LA with 12% meso-LA at ambient pressure and 105−115 °C.[6] It suggests that the crystallizability of PLLA is higher in the presence of compressed CO_2 than at ambient pressure regardless of the crystallization temperatures.

Crystal Form of Crystallized Samples. PLLA is a semicrystalline polymer possessing polymorphism. The α form is the most common and stable polymorph of PLLA, which can be obtained by crystallization from the molten or glassy state at high crystallization temperature, while a disordered α′ form is developed at low crystallization temperature by normal thermal treatment.[9−11,50,55,56] Both the α and α′ forms have a 10_3 helical chain conformation,[11,56] and the latter having loose chain packing in crystals can transform into the former at elevated temperatures.[12,55,56] Recently, another disordered crystal modification of α form (α″ form) was suggested for the crystallized PLLA with high optical purity after treatment with CO_2 at 3−15 MPa and 0−30 °C.[33]

XRD is used in this study to investigate the polymorphous behavior of samples because the α crystals of PLLA exhibits more subtle XRD pattern than the disorder one. Figure 6 shows the XRD patterns of samples after treatment in CO_2 at 2 MPa and different T_{tr}s. The result of untreated sample is also presented for comparison. The assignment of diffraction peaks is based on the reported crystal structure for the α form of PLLA.[4] Two strong diffractions, corresponding to (110)/(200) and (203), are observed at 2θ values of 16.6° and 18.9° for all crystallized samples, respectively. The (004)/(103) and (204) diffractions, which are absent in the α′ form, can be seen at 12.3° and 20.5°, respectively. Moreover, two characteristic diffractions of the α form of PLLA, attributed to (206) at 25.1° and (016) at 23.8°, are present instead of the characteristic diffractions of the α′ form of PLLA at 24.5°.[11] Therefore, the α crystal can be induced in PLLA samples uniquely by compressed CO_2 at 2 MPa and temperature as low as 65 °C.

For optically pure PLLA, the α form was reported to develop in the crystallization at ambient pressure and at temperatures higher than 100 °C and become predominant at temperatures higher than 120 °C. In this study, the as-molded amorphous sample treated at ambient pressure and 95 °C for 2 h also exhibits typical diffractions of the α form in XRD pattern (Figure S3 in the Supporting Information). The result suggests that the optical purity influences the temperature range to produce the α crystals, which would be extended to low temperature. In contrast, the molecular weight of PLLA was reported to have no effect on the respective crystallization temperature ranges to form the α′ and α crystals, although it influenced the crystallization rate significantly.[11] Both the high-pressure CO_2 and the low optical purity account for the formation of the α form of PLLA in a wide rage of treatment temperatures under compressed CO_2, which need further investigation.

It is well-known that a small exotherm, attributed to the solid phase transition from α′ to α form, exists just before the main melting peak in DSC curves for the crystallized PLLA samples containing α′ crystals.[11,50,55] However, PLLA2−65 having initial crystal form of α also exhibits a broad and weak exothermic peak between P_1 and P_2 with the peak temperature at 106.2 °C, when the heating rate was decreased to 5 °C/min shown in Figure 3a. The cold crystallization process could be responsible for the exotherm. PLLA2−65 had a low initial crystallinity, and the cold crystallization of amorphous phase became possible at a slower heating because the polymer chains had enough time to develop into crystals. The cold crystallization of PLLA2−65 was obstructed at a higher heating rate, namely 10 °C/min in this study.

The TMDSC results shown in Figure 4 confirm the existence of exothermic cold crystallization peak. For PLLA2−65, there is a big and broad exothermic peak in the nonreversible curve in the range from 90 to 130 °C, attributed to the signals of cold crystallization. The nonreversible exotherm overlaps with the nonreversible endothermic signals corresponding to annealing peak to make the latter invisible. Moreover, the reversible endothermic melting signals beginning at about 100 °C cannot offset the nonreversible cold crystallization signals, resulting in an obvious cold crystallization peak in total heat flow curve. On the other hand, the TMDSC nonreversible heat flow curve for PLLA4−65, as shown in Figure 4b, also indicates the cold crystallization process with small intensity, although the standard DSC curves for PLLA4−65 display no exotherm at heating rates from 5 °C/min to 40 °C/min, as shown in Figure 3b.

In addition, there is an obvious endothermic peak attributed to enthalpy relaxation in physical aging around the glass transition region[57] for all samples except the quenched one (Figure 1), which is absent in PLLA with high optical purity after treatment by compressed CO_2.[32,33] This peak is related to the thermal history before the DSC measurements. In order to ensure the total desorption of CO_2, all treated samples were kept at ambient conditions after treatment for about 2−3 weeks as well as the untreated one. On the other hand, the presence of enthalpy relaxation peak means considerable amorphous regions existing in the treated samples. The peak temperature of enthalpy relaxation and enthalpy loss for physical aging are included in the Supporting Information, Table S1.

Amorphous Samples after Treatment. According to their low crystallinity, three samples, i.e., PLLA2−50, PLLA2−35, and PLLA2−0, having high transparency by visual inspection, were regarded to be amorphous after treatment.

As shown in Figure 1a, PLLA2−50 only exhibits small double endothermic peaks at about 127.4 and 138.2 °C, respectively, with a crystallinity of 2.2%. It was reported that the T_g of PLLA in the presence of 2.0 MPa of CO_2 was reduced about 7.3 °C, measured by using high-pressure DSC.[19] Therefore, the insufficient crystallization of PLLA2−50 was due to the short time period for induced crystallization in compressed CO_2 at a temperature just above the plasticized T_g.

As expected, PLLA2−35 exhibits thermal behavior similar to the amorphous untreated sample because of the PLLA being in the glassy state during treatment in compressed CO_2. There is only a very small endothermic peak above the enthalpy relaxation peak during heating in DSC, indicating

almost no crystallinity induced by compressed CO_2 at 2 MPa and 35 °C.

PLLA2−0 exhibits a broad exothermic peak around 111 °C attributed to the cold crystallization of PLLA and an endothermic melting peak around 137 °C during heating in DSC. However, similar area for the two peaks suggests that PLLA2−0 was also amorphous before DSC measurement. The cold crystallization temperature is higher than the typical values ranged from 95 to 110 °C for amorphous optically pure PLLA.[13] It is consistent with the results of Tsuji and Ikada[3] that the cold crystallization temperature for amorphous PLLA increased with decreasing their optical purity. Although being amorphous, PLLA2−0 displays DSC curve totally different with those of PLLA2−35 and PLLA2−50. The big cold crystallization peak means that lots of nuclei were present in the sample, which would reduce the energy barrier for crystal growth to facilitate crystallization during heating.

There are two possible explanations for the cold crystallization peak shown in the DSC curve for PLLA2−0. One is based on the assumption that the sample was in the glassy state during treatment in CO_2 due to the low T_{tr}. It is suggested that the microstructure rearrangements of polymer occurred during the physical aging process are similar to those during crystallization induction period.[13] Therefore, local ordered domains might be expected to preform in PLLA sample during treatment and subsequent storage, which would significantly shorten crystallization induction period, accelerate the nucleation process, and consequently facilitate the cold crystallization of polymer in the DSC heating scan. Similarly, PLLA2−35 would exhibit more obvious cold crystallization peak because higher T_{tr} would promote the microstructure rearrangements of polymer. However, it was in disagreement with the DSC results, indicating the assumption is incorrect.

Actually, PLLA2−0 became opaque after compressed CO_2 treatment followed by rapid quench of pressure. Lots of microcells were formed, which was confirmed by SEM (Figures S4 and S5 in the Supporting Information), indicating that the PLLA was in the rubbery state during treatment by CO_2 at 2 MPa and 0 °C. By comparison, PLLA2−35 obtained by quickly depressurizing remained transparent and could not be foamed even in a water bath of 40 °C. Therefore, it is interesting to note that a glassy to rubbery state transition occurred with increasing T_{tr} from 35 to 50 °C and decreasing T_{tr} from 35 to 0 °C under CO_2 at 2 MPa. This effect termed retrograde vitrification is a unique phenomenon for several polymer−gas systems,[15,58−61] which is a result of rapid increase of gas solubility in polymer at low temperature. As far as we know, the retrograde vitrification behavior has never been reported in the PLLA−CO_2 system. However, this result is not surprising because the carbonyl groups in PLLA chains have favorable interaction with CO_2, which is similar to the well-studied poly(methyl methacrylate) exhibiting retrograde vitrification behavior.[15,58,59] Accordingly, the degree of supercooling below T_m for crystallization was much higher at T_{tr} = 0 °C than at 50 °C under CO_2 at 2 MPa, resulting in high driving force for nucleation to form plentiful crystal nuclei. During heating in DSC, PLLA2−0 performed cold crystallization from these crystal nuclei as soon as the polymer chains had enough mobility.

Marubayashi et al.[33] reported that PLLA can crystallize by treatment under CO_2 at 3 MPa and temperatures ranged from 0 to 40 °C for 2 h. The combination of the results shown above and in the literature suggests that the T_g−pressure envelop for retrograde vitrification of PLLA has a peak pressure with value between 2 and 3 MPa. The schematic illustration of retrograde envelop for PLLA is included in the Supporting Information, Figure S6. It is suggested that the physical state of PLLA treated under CO_2 at 2 MPa depends on the temperature, while the PLLA−CO_2 system behaves like a rubber at 3 MPa and above, irrespective of temperature because the conditions are in the rubbery region. The behavior of retrograde vitrification is useful to prepare nanocellular foams in polymer foaming.[59,61]

Accordingly, three amorphous samples, PLLA2−50, PLLA2−35, and PLLA2−0, exhibit distinct crystallization behavior during heating scan, indicating their different microstructure formed during compressed CO_2 treatment.

Conclusions

PLLA having L-isomer content of 94%, which has stereosequence structure similar to the random copolymer of L-LA with 12% meso-LA, was treated under compressed CO_2 at 2−16 MPa and 0−95 °C for 2 h. Then these treated samples were characterized by standard DSC and TMDSC to investigate the thermal behavior after CO_2 totally diffusing out. It was shown that the crystallization of PLLA is accelerated in the presence of CO_2 by comparison with ambient condition. Therefore, this PLLA possessing low crystallizability is induced to crystallize after treatment under CO_2 at 2 MPa and $T_{tr} \geq 65$ °C or higher pressures and all temperatures studied. At 2 MPa, the α crystal form is formed predominantly in the crystallized samples. Moreover, the results suggested that the crystalline phase obtained has less perfection and low crystallinity regardless of the treatment conditions. Consequently, the treated PLLA exhibited rich thermal transition signals during the DSC heating run, which is differ from the PLLA having higher L-isomer content.

Besides the endothermic enthalpy relaxation peak displayed in all treated samples, up to three endotherms and one exotherm were observed above T_g depending on the treatment condition and the heating rate. The endothermic annealing peak, P_1, is assigned to the nonreversible relaxation of rigid amorphous phase formed during CO_2 treatment, which has small intensity and shifts to high temperature with increasing treatment temperature, pressure, and DSC heating rate. The double melting peaks, P_2 and P_3, are originating from melting−recrystallization process. P_2 is attributed to the melting of original crystals presented in the crystallized sample and P_3 to the melting of recrystallized crystals with higher stability formed during heating. Compared to those of analogue crystallized under ambient pressure, the endothermic peaks have similar peak temperatures and bigger entropies. The intensity ratio of P_2 to P_3 increases with treatment temperature, pressure, and DSC heating rate. The exothermic peak relates to a cold crystallization process because of the significant fraction of amorphous phase presented in the treated sample. This peak appears between P_1 and P_2 especially in the DSC curve at a low heating rate, as the molecular chain has enough time to form crystalline structure. On the other hand, the behavior of retrograde vitrification for the PLLA−CO_2 system was revealed from the thermal behavior and foaming result of the treated samples by compressed CO_2. Therefore, PLLA is in the glassy state in the presence of CO_2 at 2 MPa and 35 °C while in the rubbery state at all pressures studied and temperature as low as 0 °C.

Acknowledgment. This work was supported by the National Natural Science Foundation of China, Grant No. 20774106, the Swedish Research Council, and the SIDA/SAREC Asian-Swedish Research Links Programme.

Supporting Information Available: ^{1}H NMR spectrum, TGA results, SEM micrograph, data for enthalpy relaxation

peak, and schematic representation of retrograde envelop. This material is available free of charge via the Internet at http://pubs.acs.org.

References and Notes

(1) Vasanthakumari, R.; Pennings, A. J. *Polymer* **1983**, *24*, 175–178.
(2) Tsuji, H.; Ikada, Y. *Polymer* **1995**, *36*, 2709–2716.
(3) Tsuji, H.; Ikada, Y. *Macromol. Chem. Phys.* **1996**, *197*, 3483–3499.
(4) Miyata, T.; Masuko, T. *Polymer* **1997**, *38*, 4003–4009.
(5) Miyata, T.; Masuko, T. *Polymer* **1998**, *39*, 5515–5521.
(6) Huang, J.; Lisowski, M. S.; Runt, J.; Hall, E. S.; Kean, R. T.; Buehler, N.; Lin, J. S. *Macromolecules* **1998**, *31*, 2593–2599.
(7) Cartier, L.; Okihara, T.; Ikada, Y.; Tsuji, H.; Puiggali, J.; Lotz, B. *Polymer* **2000**, *41*, 8909–8919.
(8) Pan, P. J.; Zhu, B.; Inoue, Y. *Macromolecules* **2007**, *40*, 9664–9671.
(9) Kawai, T.; Rahman, N.; Matsuba, G.; Nishida, K.; Kanaya, T.; Nakano, M.; Okamoto, H.; Kawada, J.; Usuki, A.; Honma, N.; Nakajima, K.; Matsuda, M. *Macromolecules* **2007**, *40*, 9463–9469.
(10) Pan, P. J.; Inoue, Y. *Prog. Polym. Sci.* **2009**, *34*, 605–640.
(11) Pan, P. J.; Kai, W. H.; Zhu, B.; Dong, T.; Inoue, Y. *Macromolecules* **2007**, *40*, 6898–6905.
(12) Pan, P. J.; Zhu, B.; Kai, W. H.; Dong, T.; Inoue, Y. *Macromolecules* **2008**, *41*, 4296–4304.
(13) Pan, P. J.; Liang, Z.; Zhu, B.; Dong, T.; Inoue, Y. *Macromolecules* **2008**, *41*, 8011–8019.
(14) Chow, T. S. *Macromolecules* **1980**, *13*, 362–364.
(15) Condo, P. D.; Johnston, K. P. *J. Polym. Sci., Part B: Polym. Phys.* **1994**, *32*, 523–533.
(16) Handa, Y. P.; Kruus, P.; Oneill, M. *J. Polym. Sci., Part B: Polym. Phys.* **1996**, *34*, 2635–2639.
(17) Zhang, Z. Y.; Handa, Y. P. *Macromolecules* **1997**, *30*, 8505–8507.
(18) Mi, Y.; Zheng, S. *Polymer* **1998**, *39*, 3709–3712.
(19) Takada, M.; Hasegawa, S.; Ohshima, M. *Polym. Eng. Sci.* **2004**, *44*, 186–196.
(20) Bratton, D.; Brown, M.; Howdle, S. M. *Macromolecules* **2003**, *36*, 5908–5911.
(21) Yoda, S.; Bratton, D.; Howdle, S. M. *Polymer* **2004**, *45*, 7839–7843.
(22) Ganapathy, H. S.; Hwang, H. S.; Jeong, Y. T.; Lee, W. K.; Lim, K. T. *Eur. Polym. J.* **2007**, *43*, 119–126.
(23) Matsuyama, K.; Zhang, D. H.; Urabea, T.; Mishima, K. *J. Supercrit. Fluids* **2005**, *33*, 275–281.
(24) Chen, A. Z.; Li, Y.; Chau, F. T.; Lau, T. Y.; Hu, J. Y.; Zhao, Z.; Mok, D. K. W. *Acta Biomater.* **2009**, *5*, 2913–2919.
(25) Meziani, M. J.; Pathak, P.; Wang, W.; Desai, T.; Patil, A.; Sun, Y. P. *Ind. Eng. Chem. Res.* **2005**, *44*, 4594–4598.
(26) Wang, X. X.; Li, W.; Kumar, V. *Biomaterials* **2006**, *27*, 1924–1929.
(27) Ema, Y.; Ikeya, M.; Okamoto, M. *Polymer* **2006**, *47*, 5350–5359.
(28) Liao, X.; Nawaby, A. V.; Whitfield, P.; Day, M.; Champagne, M.; Denault, J. *Biomacromolecules* **2006**, *7*, 2937–2941.
(29) Zhai, W. T.; Ko, Y.; Zhu, W. L.; Wong, A. S.; Park, C. B. *Int. J. Mol. Sci.* **2009**, *10*, 5381–5397.
(30) Mihai, M.; Huneault, M. A.; Favis, B. D. *J. Appl. Polym. Sci.* **2009**, *113*, 2920–2932.
(31) Yu, L.; Liu, H. S.; Dean, K.; Chen, L. *J. Polym. Sci., Part B: Polym. Phys.* **2008**, *46*, 2630–2636.
(32) Yu, L.; Liu, H.; Dean, K. *Polym. Int.* **2009**, *58*, 368–372.
(33) Marubayashi, H.; Akaishi, S.; Akasaka, S.; Asai, S.; Sumita, M. *Macromolecules* **2008**, *41*, 9192–9203.
(34) Hirota, S.-i.; Sato, T.; Tominaga, Y.; Asai, S.; Sumita, M. *Polymer* **2006**, *47*, 3954–3960.
(35) Zhai, W. T.; Yu, J.; Ma, W. M.; He, J. S. *Macromolecules* **2007**, *40*, 73–80.
(36) Ma, W. M.; Zhai, W. T.; Yu, J.; He, J. S. *Polym. Int.* **2007**, *56*, 1298–1304.
(37) Kolstad, J. J. *J. Appl. Polym. Sci.* **1996**, *62*, 1079–1091.
(38) Thakur, K. A. M.; Kean, R. T.; Hall, E. S. *Anal. Chem.* **1997**, *69*, 4303–4309.
(39) Fischer, E. W.; Sterzel, H. J.; Wegner, G. *Kolloid Z. Z. Polym.* **1973**, *251*, 980–990.
(40) Abe, H.; Harigaya, M.; Kikkawa, Y.; Tsuge, T.; Doi, Y. *Biomacromolecules* **2005**, *6*, 457–467.
(41) Baratian, S.; Hall, E. S.; Lin, J. S.; Xu, R.; Runt, J. *Macromolecules* **2001**, *34*, 4857–4864.
(42) Xu, H.; Ince, B. S.; Cebe, P. *J. Polym. Sci., Part B: Polym. Phys.* **2003**, *41*, 3026–3036.
(43) Xu, H.; Cebe, P. *Macromolecules* **2004**, *37*, 2797–2806.
(44) Liu, T.; Petermann, J. *Polymer* **2001**, *42*, 6453–6461.
(45) Bonnet, M.; Rogausch, K. D.; Petermann, J. *Colloid Polym. Sci.* **1999**, *277*, 513–518.
(46) Schwarz, I.; Stranz, M.; Bonnet, M.; Petermann, J. *Colloid Polym. Sci.* **2001**, *279*, 506–512.
(47) Reading, M. *Trends Polym. Sci.* **1993**, *1*, 248–253.
(48) Okazaki, I.; Wunderlich, B. *Macromol. Rapid Commun.* **1997**, *18*, 313–318.
(49) Okazaki, I.; Wunderlich, B. *Macromolecules* **1997**, *30*, 1758–1764.
(50) Yasuniwa, M.; Sakamo, K.; Ono, Y.; Kawahara, W. *Polymer* **2008**, *49*, 1943–1951.
(51) Lee, Y. C.; Porter, R. S. *Macromolecules* **1987**, *20*, 1336–1341.
(52) Lee, Y. C.; Porter, R. S.; Lin, J. S. *Macromolecules* **1989**, *22*, 1756–1760.
(53) Lian, Z. Y.; Epstein, S. A.; Blenk, C. W.; Shine, A. D. *J. Supercrit. Fluids* **2006**, *39*, 107–117.
(54) Fujiwara, T.; Yamaoka, T.; Kimura, Y.; Wynne, K. J. *Biomacromolecules* **2005**, *6*, 2370–2373.
(55) Zhang, J. M.; Tashiro, K.; Tsuji, H.; Domb, A. J. *Macromolecules* **2008**, *41*, 1352–1357.
(56) Zhang, J. M.; Duan, Y. X.; Sato, H.; Tsuji, H.; Noda, I.; Yan, S.; Ozaki, Y. *Macromolecules* **2005**, *38*, 8012–8021.
(57) Hutchinson, J. M. *Prog. Polym. Sci.* **1995**, *20*, 703–760.
(58) Condo, P. D.; Sanchez, I. C.; Panayiotou, C. G.; Johnston, K. P. *Macromolecules* **1992**, *25*, 6119–6127.
(59) Handa, Y. P.; Zhang, Z. Y. *J. Polym. Sci., Part B: Polym. Phys.* **2000**, *38*, 716–725.
(60) Pham, J. Q.; Johnston, K. P.; Green, P. F. *J. Phys. Chem. B* **2004**, *108*, 3457–3461.
(61) Nawaby, A. V.; Handa, Y. P.; Liao, X.; Yoshitaka, Y.; Tomohiro, M. *Polym. Int.* **2007**, *56*, 67–73.